

SUSY darkmatter at the LHC - 7 TeV

Nabanita Bhattacharyya^{(a)1}, Amitava Datta^{(a)2} and Sujoy Poddar^{(b)3}

^(a) *Indian Institute of Science Education and Research, Kolkata,
Mohanpur Campus, PO: BCKV Campus Main Office,
Mohanpur - 741252, Nadia, West Bengal.*

^(b) *Netaji Nagar Day College,
170/436, N.S.C. Bose Road, Kolkata - 700 092, India.*

Abstract

We have analysed the early LHC signatures of the minimal supergravity (mSUGRA) model. Our emphasis is on the 7 - TeV run corresponding to an integrated luminosity of $\sim 1.0 fb^{-1}$ although we have also discussed briefly the prospects at LHC-10 TeV . We focus on the parameter space yielding relatively light squark and gluinos consistent with the darkmatter relic density data and the LEP bounds on the lightest Higgs scalar mass. This parameter space is only allowed for non-vanishing trilinear soft breaking term A_0 . A significant region of the parameter space with large to moderate negative values of A_0 consistent with the stability of the scalar potential and relic density production via neutralino annihilation and/or neutralino - stau coannihilation yields observable signal via the jets + missing transverse energy channel. The one lepton + jets + missing energy signal is also viable over a smaller but non-trivial parameter space. The ratio of the size of the two signals - free from theoretical uncertainties - may distinguish between different relic density generating mechanisms. With efficient τ -tagging facilities at 7 TeV the discriminating power may increase significantly. We also comment on other dark matter relic density allowed mSUGRA scenarios and variants there of in the context of LHC-7 TeV .

PACS no:12.60.Jv, 95.35.+d, 13.85.-t, 04.65.+e

¹nabanita@iiserkol.ac.in

²adatta@iiserkol.ac.in

³sujoy_phy@iiserkol.ac.in

1 Introduction

The attention of the high energy physics community has been focussed on the prospects of new physics search at the CERN Large Hadron Collider (LHC) [1]. It is gratifying to note that the proton -proton collisions with stable beams is now operational at an energy ($\sqrt{s} = 7 \text{ TeV}$) never attained by any accelerator before. It was of course expected that before operating at the maximum attainable energy of $\sqrt{s} = 14 \text{ TeV}$, the warming up exercises will begin with low energy and low luminosity runs. However, due to the unfortunate accident which delayed the programme for about a year, the LHC operations has taken some unexpected twists and turns. For example, until a couple of months ago it was planned that a substantial amount of data will be delivered at $\sqrt{s} = 10 \text{ TeV}$ and several analyses on new physics research have been published [2]. However, a very recent revised decision has opted for data taking for the next 18 - 24 months at $\sqrt{s} = 7 \text{ TeV}$ the anticipated integrated luminosity being of the order of 1 fb^{-1} . In some very recent analyses [3] supersymmetry (SUSY) searches at $\sqrt{s} = 7 \text{ TeV}$ have also been performed. Although this is a temporary set back for the new physics search programme, it is worthwhile to check what can be achieved at $\sqrt{s} = 7 \text{ TeV}$. In this paper we concentrate on SUSY [4] search within the framework of the simplest gravity mediated supersymmetry breaking model - the minimal supergravity [5](mSUGRA) model - with the parameter space constrained by the dark matter relic density data [6].

In the mSUGRA model there are only five free parameters [5] namely a common scalar mass (m_0), a common gaugino mass ($m_{1/2}$), $\tan\beta$, A_0 and sign of μ . Here $\tan\beta$ is the ratio of the vacuum expectation values of the two neutral Higgs bosons in the model, A_0 is the trilinear soft breaking term and μ is the higgsino mass parameter; the magnitude of μ is fixed by the radiative electroweak symmetry breaking (EWSB) condition [7].

It is obvious that the strongly interacting squarks and gluinos are the species most likely to show up under the LHC microscope provided they are relatively light with masses just beyond the reach of Tevatron Run II or little more. We recall that the current lower limits [8] obtained by the CDF collaboration are 392 GeV for squark masses assuming squark and gluino masses to be approximately equal and 280 GeV for gluino masses with $m_{\tilde{q}} \gtrsim 600 \text{ GeV}$, in the mSUGRA scenario with $A_0 = 0$, $\mu > 0$ and $\tan\beta = 5$. Similar limits from the DØ collaboration [9] on the gluino mass are 379 GeV and 307 GeV respectively within the framework of mSUGRA.

The low $m_0 - m_{1/2}$ region of the parameter space yields light squarks and gluinos. This

parameter space also predicts light sleptons which facilitates neutralino pair annihilation (or bulk annihilation) [10, 11] via slepton exchange leading to dark matter (DM) relic density consistent with data.

On the other hand a significant region of the above parameter space is strongly disfavoured by the lower bound on the lightest Higgs boson mass ($m_h > 114.5 \text{ GeV}$) from Large Electron Positron (LEP) [12]. This leads to the belief that bulk annihilation cannot be an important relic density producing mechanism.

It has been pointed out [13] that the above conclusion is an artifact of the ad hoc assumption that the trilinear soft breaking parameter $A_0 = 0$, which has been invoked by most of the existing analyses [14]. On the other had for a reasonably large negative value of A_0 , which does not violate the charge colour breaking condition [15], the LEP bound on m_h can be satisfied with smaller values of m_0 and $m_{\frac{1}{2}}$ which are excluded for $A_0 = 0$. In the presence of large negative A_0 , two interesting zones (referred to as I and II) of the parameter space consistent with both Wilkinson Microwave Anisotropy Probe (WMAP) [6] and LEP data [12] open up:

I) In this zone with large negative A_0 bulk annihilation [11] is the dominant DM producing mechanism although LSP- $\tilde{\tau}$ coannihilation [16] has a significant presence.

II) In this region in contrast to Region I, LSP- $\tilde{\tau}$ coannihilation dominates while bulk annihilation produces a moderate but non-negligible fraction of the relic density. Even if LSP- $\tilde{\tau}$ coannihilation is the only significant DM producing mechanism, it may occur for smaller values of $m_{\frac{1}{2}}$ compared to the $|A_0| = 0$ case. This allows lighter squarks and gluinos.

Several examples of the above two zones are contained in Figs. 1 - 4 of [13]. In order to study the characteristic LHC signals corresponding to different relic density producing mechanism the representative points A (zone I) and B (zone II; see Table 1 reproduced from [13]) are introduced. In order to compare with the signatures corresponding to the conventional parameter space with $A_0 = 0$, a third point C is also considered. This point corresponds to the minimal value of $m_{1/2}$ for $m_0 = 120 \text{ GeV}$ consistent with the WMAP data. The expected event characteristics at the LHC for different representative points will be summarized in section 2.

It was further shown in [13] that the lepton flavour (e, μ, τ) content of the final states arising from squark-gluino events at the LHC, will be very different in the above cases. Tagging of b -jets may further help to discriminate among scenarios. The observability of the

these signals at the LHC ($\sqrt{s} = 14 \text{ TeV}$) has been illustrated [13, 17] by Pythia [18] based analyses. The τ -jet and b -jet tagging efficiencies reported by the CMS collaboration [19] were used (see Table IX of [17]). However, the flavour tagging efficiencies at $\sqrt{s} = 7 \text{ TeV}$ are not yet known. Hence the flavour tagging can not be readily employed for assessing the physics potential of the low energy runs.

It is indeed gratifying to note that generic SUSY signals consisting of m -leptons + n -jets + \cancel{E}_T without any flavour tagging also differ dramatically in the above three scenarios [17] (see Table IV). The main purpose of this paper is to scrutinize different relic density producing mechanisms and check the feasibility of distinguishing among them by using these generic signals at LHC runs at energies lower than the maximum attainable one. It should be stressed that the parameter space studied in this paper and its physical significance in the context of SUSY dark matter is totally different from the other studies [3].

At the focus of our attention is the physics at $\sqrt{s} = 7 \text{ TeV}$ (section 3). However, the strategy for future runs at the LHC will depend on the performance of the experiments at 7 TeV . Another round of experiments at an energy lower than the maximum attainable energy is cannot not be ruled out as yet. We have, therefore, briefly discussed the signatures of the above scenarios at $\sqrt{s} = 10 \text{ TeV}$, the proposed energy for the preliminary runs until very recently (section 4).

Although we have focussed on the benchmark points A, B and C, we have also considered several other points consistent with the relic density data. These points belong to different regions of the parameter space yielding distinct sparticle spectra and collider signatures. The points A, B and C are chosen with $\tan\beta = 10$. In this analysis the allowed points at higher as well as lower values of $\tan\beta$ have been considered to make the study more comprehensive (section 3). Using reasonable guesses about the efficiency, we have also considered the prospect of observing τ -jet tagged signals at the low energy runs at $7 - \text{TeV}$. We have also taken this opportunity to improve some of our earlier background estimates in [13, 17].

Other authors have also proposed schemes for testing the origin of dark matter production at the LHC [20].

2 The allowed mSUGRA parameter space for non zero trilinear soft breaking terms

In [13] signals at the LHC corresponding to the WMAP allowed regions of the parameter space with non-zero A_0 were studied at 14 TeV . The results were compared and contrasted with the expectations from the well publicized conventional $\tilde{\tau}_1$ -coannihilation [10, 16] scenario with $A_0 = 0$ by introducing three benchmark points A, B and C. The corresponding mSUGRA parameters are reproduced in Table 1 for ready reference.

mSUGRA parameters	A	B	C
m_0	120.0	120.0	120.0
$m_{1/2}$	300.0	350.0	500.0
A_0	-930.0	-930.0	0.0
$\tan \beta$	10.0	10.0	10.0
$sign(\mu)$	1.0	1.0	1.0

Table 1: Three bench mark scenarios introduced in [13]. All parameters with dimension of mass are in GeV .

The sparticle spectra in the three scenarios can be found in Table II of [13]. The total cross section of squark gluino events decreases significantly as we go from A to C, which is easily understood from the respective sparticle spectra. In scenario A the lighter top squark-antisquark ($\tilde{t}_1\tilde{t}_1^*$) pair production enhances the total cross section significantly. This is a direct consequence of large negative A_0 . This trend is also seen at 7 - TeV (see Table 2).

The signals at the LHC are governed by the cascade decays of the sparticles. In all three cases the gluinos being heavier than all squarks, decay into quark-squark pairs (Table III of [13]). Decays into $t - \tilde{t}_1$ pairs dominate in scenarios A and B (Table IV of [13]), as the third generation squarks are relatively light due to the renormalization group evolution and large $|A_0|$.

The squarks in general decay into the corresponding lighter quarks and an appropriate

electroweak gaugino. The decay of each third generation squark inevitably contains a bottom (b) quark. This is the origin of the large fraction of final states with b -jets as noted in [13]. In scenario C the fraction of third generation squarks in gluino decay is relatively small and the above effect is suppressed.

The decay properties of the lighter chargino ($\tilde{\chi}_1^\pm$) and the second lightest neutralino ($\tilde{\chi}_2^0$) which, in addition to the LSP, are often present in squark-gluino decay chains control the lepton content of the final states to a large extent. As a direct consequence of the presence of the light sleptons, these two unstable gauginos decay almost exclusively into leptonic channels via two body modes in all three scenarios. In scenario A the lighter chargino decays into R-type sleptons with a large BR. This results in a very large fraction of final states containing the $\tilde{\tau}_1$ which is always lighter than the other sleptons and eventually decays into a τ -LSP pair (see Table V of [13] and Table II of [17]). The $\tilde{\chi}_2^0$ decays primarily into τ - $\tilde{\tau}_1$ pair contributing further to the τ dominance in the final states. The scenario B has all the above features albeit to a lesser extent. In scenario C the $\tilde{\chi}_1^\pm$ decays into left slepton- neutrino pairs or sneutrino-lepton pairs of all generations with almost equal BR of sizable magnitudes and lepton universality holds to a very good approximation.

3 The Signals at the LHC at 7 TeV

In this analysis we have generated all squark-gluino events at $E_{CM} = 7 \text{ TeV}$ using Pythia [18]. Initial and final state radiation, decay, hadronization, fragmentation and jet formation are implemented following the standard procedures in Pythia. The lowest order squark-gluino production cross-sections have been computed by CalcHEP [21]. The corresponding cross-sections for the scenarios A, B and C are presented in Table 2.

We have used the toy calorimeter simulation (PYCELL) provided in Pythia with the following criteria:

- The calorimeter coverage is $|\eta| < 4.5$. The segmentation is given by $\Delta\eta \times \Delta\phi = 0.09 \times 0.09$ which resembles a generic LHC detector.
- A cone algorithm with $\Delta R = \sqrt{\Delta\eta^2 + \Delta\phi^2} = 0.5$ has been used for jet finding.
- $E_{T,\min}^{\text{jet}} = 30 \text{ GeV}$ and jets are ordered in E_T .

Process	σ (pb)		
	A	B	C
$\tilde{g}\tilde{g}$	0.040	0.010	0.26×10^{-3}
$\tilde{q}_L\tilde{g}$	0.140	0.057	2.44×10^{-3}
$\tilde{q}_R\tilde{g}$	0.155	0.063	2.78×10^{-3}
$\tilde{q}_L\tilde{q}_L$	0.113	0.057	5.62×10^{-3}
$\tilde{q}_R\tilde{q}_R$	0.100	0.051	5.49×10^{-3}
$\tilde{q}_L\tilde{q}_R$	0.059	0.055	2.08×10^{-3}
$\tilde{t}_1\tilde{t}_1^*$	0.928	0.162	0.047×10^{-3}
Total	1.535	0.455	0.018

Table 2: The production cross sections of all squark-gluino events studied in this paper.

The stable leptons are selected according to the criterion :

- Leptons ($l = e, \mu$) are selected with $P_T \geq 20$ GeV and $|\eta| < 2.5$. For lepton-jet isolation we require $\Delta R(l, j) > 0.5$. For the sake of simplicity the detection efficiency of e and μ are assumed to be 100%.

The following cuts are implemented for background rejection :

- We have required two leading jets having $P_T^{j_1} > 100$ GeV and $P_T^{j_2} > 75$ GeV. (CUT 1)
- Events with missing transverse energy (\cancel{E}_T) < 350 GeV are rejected. (CUT 2)
- Events with $M_{eff} < 750$ GeV are rejected, where $M_{eff} = |\cancel{E}_T| + \sum_i |P_T^{l_i}| + \sum_i |P_T^{j_i}|$ ($l = e, \mu$). (CUT 3)
- Only events with jets having $S_T > 0.2$, where S_T is a standard function of the eigenvalues of the transverse sphericity tensor, are accepted. (CUT 4)

These cuts are motivated by the analysis of generated squark-gluino events by CMS collaboration [22] although we have relaxed some of them in view of the reduced \sqrt{s} . We begin with the generic SUSY signals of the type $m-l + n-j + \cancel{E}_T$, where $l = e$ or μ and j is any jet. For establishing these generic signals Cut 1 - Cut 4 are adequate.

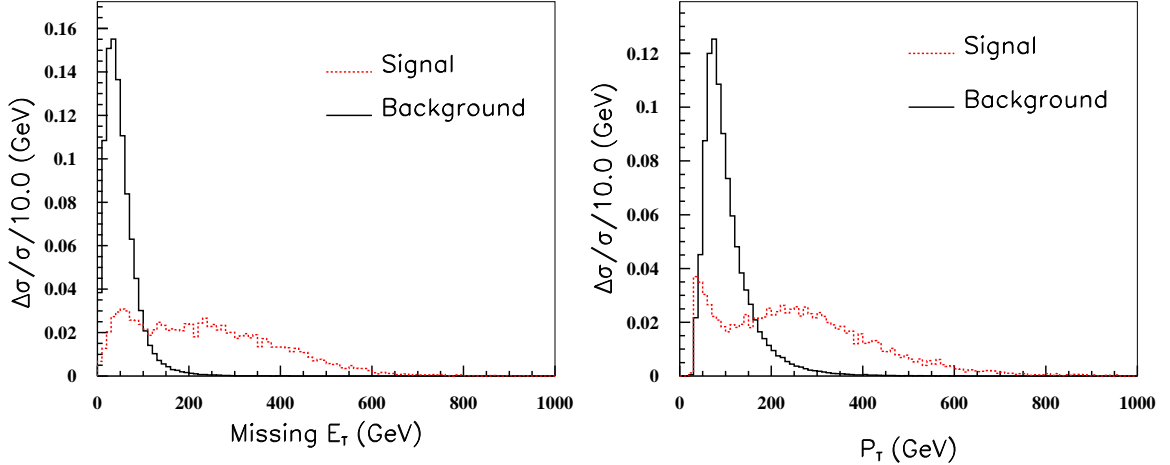


Figure 1: The distributions (normalised to unity) of \cancel{E}_T (left) and $P_T^{j_1}$ (right) for $0l$ events (before the selection cuts) for the signal (scenario A) and the dominant backgrounds.

We have considered the backgrounds from $t\bar{t}$, QCD events, $W + n\text{-jets}$ and $Z + n\text{-jets}$ events, where W and Z decays into all channels.

We have generated $t\bar{t}$ events using Pythia and the LO cross-section has been taken from CalcHEP which is 68 pb . For QCD processes generated by Pythia the contribution from the \hat{p}_T bin $400 \text{ GeV} < \hat{p}_T < 1000 \text{ GeV}$ has been considered where \hat{p}_T is defined in the rest frame of the parton parton collision. The cross-section for this bin is 227 pb . However, for other bins ($25 \text{ GeV} < \hat{p}_T < 400 \text{ GeV}$ and $1000 \text{ GeV} < \hat{p}_T < 2000 \text{ GeV}$), the background events are negligible.

For $W + n\text{-jets}$ events we have generated events with $n = 0, 1$ and 2 at the parton level using ALPGEN (v 2.13) [23]. We have generated these events subjected to the condition that $P_T^j > 60 \text{ GeV}$. These partonic events have been fed to Pythia for parton showering, hadronization, fragmentation and decays etc.

Similarly we have also generated $Z + n\text{-jets}$, events with $n = 0, 1$ and 2 using ALPGEN (v 2.13). The partonic jets have $P_T > 60 \text{ GeV}$ and fed then to Pythia for further analysis.

In Fig. 1 we have presented the normalised distributions of \cancel{E}_T (left panel) and $P_T^{j_1}$ (right panel) for $0l$ events. The dominant backgrounds are from $W + n\text{-jets}$ and $Z + n\text{-jets}$ with $n = 1$ and 2 . These distributions motivate CUT 1 and CUT 2.

For both the 1 gauge boson + n -jets backgrounds the contribution from $n = 0$ is negligible. The total background and the individual contribution of each channel to it are in Table 4. We have computed the significance $(\frac{S}{\sqrt{B}})$ for an integrated luminosity of 1 fb^{-1} where S is the number of signal events and B denotes the background events. For scenario A the significance for $0l$ and $1l$ are 13.8 and 2.8 respectively (from Tables 3 and 4). For scenario B (C) the corresponding numbers are 7.9 (0.51) and 2.19 (3.5×10^{-4}).

The sizable uncertainties in the counting rates at $\sqrt{s} = 14 \text{ TeV}$ due to the choice of the parton density functions (PDF) and the QCD scale has already been discussed (see Table III of [17]). It also follows from the same table that the ratio of two cross-sections with different m and n is remarkably stable with respect to the above uncertainties. Thus to identify a particularly relic density producing scenario unambiguously at least two measurements, for example the number of $0l$ and $1l$ events, are essential. However, the numbers in the last paragraph 3 indicate that the statistics for $1l$ events may not be adequate for $\mathcal{L} = 1 \text{ fb}^{-1}$. With a luminosity of 2 fb^{-1} the ratio $R = \frac{\sigma_{0l}}{\sigma_{1l}}$ can be measured with some confidence in scenario A. On the other hand if no signal is seen even in the $0l$ channel, point A will be strongly disfavoured in spite of the uncertainties.

In order to make the scanning more comprehensive we have scanned several points around A chosen from Fig. 1a) of [13] belonging to zone I defined in the introduction. For $m_{1/2}$ lower than that of A, the cross section of $0l$ events is huge. For example, with $m_0 = 120, m_{1/2} = 250, A_0 = -930$ we find $(\frac{S}{\sqrt{B}})_{0l} \approx 38$ at $\mathcal{L} = 1 \text{ fb}^{-1}$. All mSUGRA mass parameters are in GeV unless mentioned otherwise. Thus even the 7 - TeV run can probe bulk annihilation as a viable relic density producing mechanism for non-zero trilinear couplings or disfavour it. Similarly a large number of points in zone II around point B were scanned and $(\frac{S}{\sqrt{B}})_{0l} \gtrsim 5$ were obtained in most of the cases. However, a large part of zone II will remain unexplored at $\sqrt{s} = 7 \text{ TeV}$.

Although $(\frac{S}{\sqrt{B}})_{1l}$ is less than 5 in scenarios A and B, larger values show up in several regions allowed by relic density data and LEP bound on m_h . At these points with different values of $\tan\beta = 5, 10$ and 20 the cross sections (see Table 3 for illustrations) are significantly larger compared to A or B. As a result signal events of both $0l$ and $1l$ type are sizable at $\mathcal{L} = 1 \text{ fb}^{-1}$ and their ratio - free from theoretical uncertainties - may indicate the relic density producing mechanism. For example, at the point D (see figure 2 b) of [13]) with $m_0 = 80,$

	A	B	C	D	E	F
σ (pb)	1.535	0.465	0.018	3.2	11.3	10.3
$0l$	0.1386	0.0798	0.0051	0.125	0.316	0.287
$1l$	0.0161	0.0122	0.0020	0.0384	0.026	0.033
$1\tau + X$	0.010	0.0051	0.0003	0.005	0.024	0.015

Table 3: The cross-sections (including efficiency) at $Q = \sqrt{\hat{s}}$ for signal events with different m . For details of D, E and F see text.

	$t\bar{t}$	$W + 1j$	$W + 2j$	$Z + 1j$	$Z + 2j$	QCD	Total
σ (pb)	68	1836	446	652	122	227	Background
$0l$	0.00374	0.0129	0.0241	0.0196	0.03686	0.0043	0.1015
$1l$	0.00129	0.0165	0.0147	-	-	-	0.0328
$1\tau + X$	0.00034	0.0013	0.0024	-	0.00046	0.0015	0.006

Table 4: The cross-sections (including efficiency) at $Q = \sqrt{\hat{s}}$ for background process with different m . No entry in a particular column (-) means negligible background.

$m_{1/2} = 300$, $A_0 = -1000$, $\tan\beta = 5$, $(\frac{S}{\sqrt{B}})_{1l} \approx 7$ ⁴. For $m_0 = 100$, $m_{1/2} = 220$, $A_0 = -700$, $\tan\beta = 10$ (point E; see fig 4 of [13]), $(\frac{S}{\sqrt{B}})_{1l} \approx 5$. At the last two points bulk annihilation is the dominant generator of relic density. Finally at the point F $m_0 = 150$, $m_{1/2} = 200$, $A_0 = -600$, $\tan\beta = 20$ (not studied in [13]) the $(\frac{S}{\sqrt{B}})_{1l} \approx 6$ for \mathcal{L} of 1 fb^{-1} . As illustrated by the last point the Higgs mass bound [12] can also be satisfied for low m_0 and $m_{1/2}$ if $\tan\beta$ is large even if A_0 is smaller than the values in A or B. Many of these points are also consistent with the relic density constraint (see Fig. 3 of [13] with $\tan\beta = 30$). The allowed points yield observable $0l$ signal but $1l$ signal is difficult to observe. This is due to the fact that most of the final states arising from electroweak gaugino decays contain τ 's rather than e and/or μ . For example, with $m_0 = 170$, $m_{1/2} = 370$, $A_0 = -100$, $\tan\beta = 30$ the $(\frac{S}{\sqrt{B}})_{0l} \approx 6$ for \mathcal{L} of 1 fb^{-1} . However, the $1l$ signal is unobservable.

⁴At this point the predicted Higgs mass is little smaller than the LEP bound. However, due to the uncertainty of about 3 GeV [24] in the predicted m_h this point is acceptable.

It bears recall that the number of final states with tagged τ -jets differs dramatically in the scenarios A, B and C [13, 17]. We, therefore, turn our attention to final states of the type $1\tau + X$, where X includes two or more hard jets but no e or μ or tagged τ .

In ref. [17] τ -jets with $P_T^{\tau-jet} > 30 \text{ GeV}$ and $|\eta| < 3.0$ were shown to be taggable according to the efficiencies quoted by the CMS collaboration for different P_T bins (see Fig. 12.9 of [19]). For $P_T \geq 130 \text{ GeV}$ the tagging efficiency was as high as 0.90 while for softer jets the efficiencies were considerably smaller (e.g., 0.50 for $30 \text{ GeV} \leq P_T \leq 50 \text{ GeV}$). However, for 7 TeV runs such information is not available. As a reasonable guess we have assumed the overall τ -jet tagging efficiency to be 50% for $P_T^{\tau-jet} > 30 \text{ GeV}$ and $|\eta| < 3.0$. The number of $1\tau + X$ events for $\mathcal{L} = 1 \text{ fb}^{-1}$ for signal A, B and C turn out to be 10, 5 and 0.12 respectively. The other cuts are as stated above. The total number of background events from the sources in Table 4 is 6. The background from QCD arises due to mistagging of light jets. A mistagging probability of 3% has been assumed for jets with $P_T > 30 \text{ GeV}$. Considering this efficiency for scenario A the significance for $1\tau + X$ becomes 4.1 for $\mathcal{L} = 1 \text{ fb}^{-1}$. For scenarios B and C the signal has poor significance. Thus if τ -jet tagging can be implemented more efficiently and/ or the accumulated luminosity is larger than $\mathcal{L} = 1 \text{ fb}^{-1}$, then $1\tau + X$ events may provide another handle for discriminating different relic density producing scenarios.

In this paper we have worked with leading order(LO) cross section only. This is because the next to leading order (NLO) results for many of the backgrounds at 7 - TeV are not known. From [25] it is well known that the K factors for the signal events vary from 1.3 - 1.4 for different signal processes at 14 - TeV . In the third paper of [3] the K-factor of squark-gluino production cross section was estimated to be approximately 1.3. Thus even if the NLO correction enhances the total background by a factor of two, the significances of the signals studied in this paper are not likely to change dramatically.

There are other mSUGRA scenarios consistent with relatively light squark gluinos, the observed dark matter relic density and the Higgs mass bound from LEP, which could be of interest for the low energy runs of the LHC. If one considers large $\tan\beta$ ($\gtrsim 45$) the ‘Higgs funnel’ opens up [26]. Here a LSP pair annihilates into $b - \bar{b}$ through the A (the pseudo scalar Higgs) resonance to produce the observed relic density. Sometimes the H (the heavy scalar Higgs) resonance also contributes.

A part of the funnel region corresponds to light squarks and gluinos. The observability of this region for $\tan\beta = 45$ at LHC-7 TeV has been studied (see Fig. 2 of the third paper of

[3]). It follows that if one takes into account the uncertainties in the theoretical prediction of the Higgs mass (i.e., parameter spaces with $111 < m_h < 114 \text{ GeV}$ are considered to be allowed) a small domain of the parameter space consistent with WMAP data can be probed with 1 fb^{-1} of integrated luminosity.

A variation of the above theme is the "h-pole region", where the condition $2m_{\tilde{\chi}_1^0} \lesssim m_h$ is satisfied [27, 28]. Here $\tilde{\chi}_1^0$ annihilates through the exchange of a nearly on-shell light CP even Higgs boson h . We present some example from [28] within the framework of mSUGRA. Here large ranges of m_0 and A_0 are allowed but low $m_{1/2}$ is essential. This leads to strong upper bounds on $m_{\tilde{\chi}_1^+}$, $m_{\tilde{\chi}_2^0}$ and most importantly on $m_{\tilde{g}}$. Hence the scenario could be interesting for low energy runs. Some examples from [28] are

- (i) $m_t = 178 \text{ GeV}$, $m_0 = 1500 \text{ GeV}$, $A_0 = -1000 \text{ GeV}$, $\tan\beta = 30$ leading to $m_h \sim 117 \text{ GeV}$.
- (ii) $m_t = 182 \text{ GeV}$, $m_0 = 1000 \text{ GeV}$, $A_0 = -1000 \text{ GeV}$, $\tan\beta = 10$ leading to $m_h \sim 115 \text{ GeV}$.
- (iii) $m_t = 185 \text{ GeV}$, $m_0 = 1000 \text{ GeV}$, $A_0 = 0 \text{ GeV}$, $\tan\beta = 20$ leading to $m_h \sim 116 \text{ GeV}$.

In all the above cases DM allowed regions are obtained for $m_{1/2} < 145 \text{ GeV}$. Unfortunately, as already noted in [28], this resonance condition is satisfied if the physical mass of the top quark turns out to be on the higher side which was favoured by the then available data. Such high m_t are, however, disfavoured by the central value of the current data $m_t \approx 173 \text{ GeV}$.

In the mSUGRA scenario the scalars and the gaugino masses are strictly universal at the GUT scale (M_G). These conditions severely restrict the mSUGRA parameter space consistent with the observed DM relic density. If departures from the strict universality are allowed [29], new regions of the parameter space consistent with both the relic density data and light squark and gluinos open up and novel LHC signatures are predicted. Most of the above works are, however, in the context of LHC-14 TeV .

There are so many models for non-universality that we were forced to restrict ourselves, perhaps quite arbitrarily, to brief comments on two scenarios only. A dark matter allowed region can be obtained for relatively low values of M_3 (see the first paper of [29]) due to non-universal gaugino masses at M_G . For example, for $m_0 = 300 \text{ GeV}$, $M_1 = M_2 = 300 \text{ GeV}$, $M_3 = 160 \text{ GeV}$, $A_0 = 0$, $\tan\beta = 10$, $\mu > 1$ the value of $\Omega h^2 = 0.10$. Although in this region $m_h = 106 \text{ GeV}$, which is disfavoured in spite of the uncertainty in m_h noted above.

We have already argued that for negative values of A_0 , consistency with the m_h bound from LEP can be restored. Keeping all the parameters in the last paragraph fixed and taking

$A_0 = -600 \text{ GeV}$ we obtain $\Omega h^2 = 0.12$. The masses of the sparticles (in GeV) of interest are:

$$h = 112, \tilde{g} = 417, \tilde{u}_L = 494, \tilde{u}_R = 464, \tilde{t}_1 = 133, \tilde{b}_1 = 406, \\ \tilde{e}_L = 364, \tilde{e}_R = 322, \tilde{\tau}_1 = 312, \tilde{\chi}_1^+ = 216, \tilde{\chi}_2^0 = 217, \tilde{\chi}_1^0 = 119.$$

The above spectrum and the size of the signal estimated by us in this paper certainly suggest that an observable signal even at LHC-7 TeV is a distinct possibility.

There is an economical way of introducing non-universality of squark masses at M_G by introducing a single parameter - the $SO(10)$ D-term (for reference to earlier works and novel signatures at Tevatron Run II see [30, 31]. Here a possible scenario is lighter down squarks of the R-type. These squarks along with a light gluino can indeed lead to novel signals at LHC -7 TeV .

We have deliberately refrained from imposing indirect constraints on the mSUGRA parameter space, since these constraints invariably involve additional theoretical assumptions. The relaxation of such assumptions may drastically change the indirect constraints without affecting the collider signatures and the relic density calculation.

For example, the requirement that no charge colour breaking (CCB) breaking minima of the scalar potential be deeper than the EWSB vacuum (the unbounded from below (UFB)-3 constraint, the second paper of [15]), puts lower bounds on sparticle masses [32] which are stronger than the direct bounds from LEP in the mSUGRA model. However, such constraints lose their relevance if the EWSB minimum is a false vacuum with a life time larger than the age of the universe [33].

Similarly the $BR(b \rightarrow s\gamma)$ measured by the BABAR, BELLE and CLEO collaborations, is often used to constrain the underlying theory. However, the theoretical predictions have their share of uncertainties. The current data as quoted by the Heavy Flavour Averaging Group (HEFAG) is $(3.52 \pm 23 \pm 9) \times 10^{-6}$ [34]. The improved SM prediction (NLO) [35] $(3.15 \pm 0.23) \times 10^{-4}$, though consistent with the data within errors, leaves ample room for a larger positive contribution from SUSY compared to the earlier estimates. This opens up the possibility of lighter sparticles in the mSUGRA model [36]. There are additional uncertainties as well. The assumption of minimal flavour violation, which is employed in theoretical computations, is not foolproof either. The relaxation of this assumption drastically weakens the constraints [37]. Even within the minimal flavour violation the inclusion of the CP violating phases leads to further uncertainties in the theoretical prediction (see, e.g., the

second paper of [37] and references there in). It should be borne in mind that relaxation of the above assumptions will have very little or no impact on the direct collider signatures considered by us.

4 The Signals at the LHC at 10 TeV

In this section we briefly study the generic SUSY signals of the type $m-l + n-j + \cancel{E}_T$. Our aim is to study the feasibility of discriminating among the three models in Table 1, should the performance of the 7 - TeV run suggest yet another experiment at an energy less than the maximum attainable energy. To be specific we have considered a run at 10 TeV which until recently was the favoured option. The total lowest order squark-gluino production cross-sections have been computed by CalcHEP [21] and given in Table 5. We have used the same selection criterion for jets and leptons as in [17] for LHC-14 TeV . For background rejection we have used the CMS cuts which are also used in [17].

	A	B	C
σ (pb)	5.12	1.663	0.1548
$0l$	0.5628	0.3238	0.0434
$1l$	0.0488	0.0393	0.0186
SS	0.00072	0.000698	0.00134
OS	0.00154	0.002278	0.00359
$3l$	0.000051	.000133	.00066

Table 5: The cross-sections (including efficiency) at $Q = \sqrt{\hat{s}}$ for signal process with different m . Here SS refers to $m = 2$ with leptons carrying the same charge and OS refers to similar events with leptons carrying opposite charge.

In Table 5 we have shown a multi-channel analysis using signals with different choices of m (the number of leptons in the final state) which efficiently discriminate among different scenarios. We present in Table 6 the important standard model backgrounds in the leading order for $Q = \sqrt{\hat{s}}$. The $t\bar{t}$ and QCD backgrounds have been calculated in the same way as in [17]. For $W + n-jets$ and $Z + n-jets$ events we have generated events with $n = 0, 1$

	$t\bar{t}$	$W + 1j$	$W + 2j$	$Z + 1j$	$Z + 2j$	QCD	Total
σ (pb)	170	1549.5	468.1	577.9	127.6	758	Background
$0l$	0.0657	0.0638	0.1379	0.0364	0.1089	0.904	1.3167
$1l$	0.0315	0.0550	0.0944	0.00173	0.0021	0.0015	0.1862
SS	0.00017	-	-	-	-	-	0.00017
OS	0.00323	-	-	-	-	-	0.00323

Table 6: The cross-sections (including efficiency) at $Q = \sqrt{\hat{s}}$ for background process with different m . $3l$ is background free. No entry in a particular column (-) means negligible background.

	A	B	C
$0l$	49.1	28.2	3.8
$1l$	11.3	9.1	4.3
SS	5.5	5.4	10.3
OS	2.7	4.0	6.3

Table 7: The significance (S/\sqrt{B}) of signals in Table 5 for $\mathcal{L}= 10 \text{ fb}^{-1}$.

	A	B	C
σ (pb)	5.12	1.663	0.1548
$1\tau + X$	0.0663	0.0337	0.0042
$1e + X$	0.012	0.0096	0.0057

Table 8: The cross-sections (including efficiency) of events with one detected τ and one isolated e . Here X stands for all possible final states excluding any lepton or tagged τ but with at least two jets. The number of tagged b -jets is given by n - b , $n = 1, 2, 3$ (see the first column of row 4 - 9) .

	$t\bar{t}$	$W + 1j$	$W + 2j$	$Z + 1j$	$Z + 2j$	QCD	Total
σ (pb)	170	1549.5	468.1	577.9	127.6	758	Background
$1\tau + X$	0.0104	0.0087	0.0236	0.00116	0.00456	0.142	0.1904
$1e + X$	0.0095	0.0203	0.0309	0.0006	0.00035	0.0003	0.0620

Table 9: Same as Table 8 for backgrounds.

	A	B	C
$1\tau + X$	15.2	7.7	0.9
$1e + X$	4.8	3.6	2.3

Table 10: The S/\sqrt{B} ratio for the signals in Table 8 corresponding to $\mathcal{L}= 10 \text{ fb}^{-1}$.

and 2 at the parton level using ALPGEN (v 2.13) [23]. We have generated these events with $P_T^j > 80 \text{ GeV}$. These partonic events have been fed to Pythia for parton showering, hadronization, fragmentation and decays etc.

In Table 7 we have presented the significance ($\frac{S}{\sqrt{B}}$), where $S(B)$ is the total number of signal (background) events for integrated luminosity \mathcal{L} of 10 fb^{-1} .

Although the squark-gluino production cross-section is rather tiny in scenario C the signal cross-sections predicted for $m \geq 2$ is larger than the corresponding signals in A and B with much larger raw production cross-section. This again is a direct consequence of the large BRs of electroweak gaugino decays into e and μ .

From Table 7 it is clear that one way to unambiguously discriminate between A, B on the one hand and C on the other, is the count of $0l$ and $1l$ events and their ratio free from theoretical ambiguities. These signals are not visible in scenario C. In contrast the visibility of SS and OS signals in scenario C is much better. However, the observation of the almost background free signal for $m = 3$ is the best bet for establishing C since no statistically significant signal is expected from A or B in this case, although this may require $\mathcal{L} \geq 20 \text{ fb}^{-1}$.

Obviously the number of final states involving τ leptons, a critical observable for discriminating among the models, cannot be established without invoking τ -jet tagging in the

analysis. We, therefore, turn our attention to final states of the type $1\tau + X$ where X includes two or more hard jets but no e or μ or tagged τ . Tagging of τ -jets are implemented as in [17] which followed the CMS analysis.

The computation of $1e + X$ type events are rather straight forward. Here for simplicity we have assumed the e-detection efficiency to be 100 %. In our generator level analysis the result for $1\mu + X$ is expected to be the same to a good approximation and we do not present them separately. It should be borne in mind that in this case harder cuts on e has been implemented to exclude the electrons from the leptonic τ decays. The QCD background to $1\tau + X$ events stems from mistagging of light flavour jets as τ -jets. The mistagging probability has also been taken from [19] Fig. 12.9. Table 8 contains the $1\tau + X$ and $1e + X$ signals. The dominant SM backgrounds have been listed in Table 9.

The statistical significance of various signals for the representative value \mathcal{L} of 10 fb^{-1} are listed in Table 10. The $1\tau + X$ signal, if unambiguously observed, will disfavour model C.

5 Conclusions

The mSUGRA parameter space with relatively low m_0 and $m_{1/2}$ corresponding to light squarks and gluinos is consistent with the WMAP data on DM relic density and the lower bound on the lightest Higgs scalar mass from LEP, provided the trilinear coupling A_0 has large to moderate negative values [13]. Scanning the parameter space by generating squark-gluino events with the event generator Pythia we find that the jets + \cancel{E}_T signal is observable over a significant parameter space (see Tables 3 and 4 and the discussions in section 3) for an integrated luminosity of $\mathcal{L} = 1 \text{ fb}^{-1}$. In a smaller but non-trivial parameter space the $1-l + \text{jets} + \cancel{E}_T$ signal is also observable. The probability of observing the latter increases if a little larger integrated luminosity $\mathcal{L} = (2 - 3) \text{ fb}^{-1}$ is available. If both the signals are observable then the ratio of the number of events which is remarkably free from theoretical uncertainties may help distinguishing among different scenarios [17]. However, the parameter space with the conventional choice $A_0 = 0$ where LSP - $\tilde{\tau}_1$ coannihilation is the only relic density generating mechanism does not yield any observable signal.

As already noted in [13] the $1\tau + X$ signal, where X includes two or more hard jets but no e or μ or tagged τ is a very good discriminator for different mechanisms for relic density production. In the absence of any information about the τ -jet tagging efficiency at 7 - TeV

from simulations by the experimentalists, we have assumed an overall efficiency of 50% for $P_T^{\tau\text{-jet}} > 30 \text{ GeV}$ and $|\eta| < 3.0$. With this choice no observable signal emerge for $\mathcal{L} = 1 \text{ fb}^{-1}$. However, if τ -jet tagging efficiency and/or \mathcal{L} increases, then an additional handle for DM signatures at 7 - TeV will be available.

Since the performance of the 7 - TeV run may dictate yet another round of experiments at an energy less than the maximum attainable energy, we have considered the above signal at LHC-10 TeV . Here a full multichannel analysis of generic SUSY signals consisting of m -leptons + n -jets + \cancel{E}_T without any flavour tagging can probe the parameter space in great details (see Tables 5 - 7). Of course if efficient flavour tagging is available a more powerful discriminator of different relic density producing mechanisms will be in operation (see Tables 8 - 10).

Acknowledgment: NB would like to thank the Council of Scientific and Industrial Research, Govt. of India for financial support.

References

- [1] For a recent review see for example, P. Nath *et al.*, arxiv:1001.2693[hep-ph].
- [2] H. Baer, A. Lessa and H. Summy, Phys. Lett. B **674**, 49 (2009); H. Baer, V. Barger, A. Lessa and X. Tata, J. High Energy Phys. **0909**, 663 (2009); J. Edsjo, E. Lundstrom, S. Rydbeck and J. Sjolín, J. High Energy Phys. **1003**, 054 (2010); D. Feldman, G. Kane, R. Lu and B. D. Nelson, Phys. Lett. B **687**, 363 (2010); H. Baer, arXiv:1002.4155[hep-ph]; J. Dietrich *et al.* (ATLAS Collaboration), arXiv:1005.2034[hep-ph].
- [3] H. Baer, S. Kraml, A. Lessa and S. Sekmen, J. High Energy Phys. **1002**, 055 (2010); H. K. Dreiner, M. Kramer, J. M. Lindert and B. O’Leary, J. High Energy Phys. **1004**, 109 (2010); H. Baer, V. Barger, A. Lessa and X. Tata, arXiv:1004.3594[hep-ph]; The ATLAS Collaboration in the last paper of Ref[2].
- [4] For reviews on Supersymmetry, see, *e.g.*, H. P. Nilles, Phys. Rep. **110**, 1 (1984); H. E. Haber and G. Kane, Phys. Rep. **117**, 75 (1985); J. Wess and J. Bagger, *Supersymmetry and Supergravity*, 2nd ed., (Princeton, 1991); M. Drees, P. Roy and R. M. Godbole, *Theory and Phenomenology of Sparticles*, (World Scientific, Singapore, 2005).

- [5] A. H. Chamseddine, R. Arnowitt and P. Nath, Phys. Rev. Lett. **49**, 970 (1982); R. Barbieri, S. Ferrara and C. A. Savoy, Phys. Rev. Lett. **119**, 343 (1982); L. J. Hall, J. Lykken and S. Weinberg, Phys. Rev. D **27**, 2359 (1983); P. Nath, R. Arnowitt and A. H. Chamseddine, Nucl. Phys. B **227**, 121 (1983); N. Ohta, Prog. Theor. Phys. **70**, 542 (1983).
- [6] D. N. Spergel *et al.*, Astrophys. J. Suppl. **170**, 377 (2007).
- [7] L. Ibanez and G. Ross, Phys. Lett. B **110**, 215 (1982).
- [8] CDF Collaboration (T. Aaltonen *et al.*), Phys. Rev. Lett. **102**, 121801 (2009).
- [9] DØ Collaboration (T. Abazov *et al.*), Phys. Lett. B **660**, 449 (2008).
- [10] Some comprehensive review articles are G. Jungman, M. Kamionkowski and K. Greist, Phys. Rep. **267**, 195 (1996); W. L. Freedman and M. S. Turner, Rev. Mod. Phys. **75**, 1433 (2003), L. Roszkowski, Pramana **62**, 389 (2004); A. B. Lahanas, N. E. Mavromatos and D. V. Nanopoulos, Int. J. Mod. Phys. D **12**, 1529 (2003) C. Munoz, Int. J. Mod. Phys. A **19**, 3093 (2004) Manuel Drees, Plenary talk at 11th International Symposium on Particles, Strings and Cosmology (PASCOS 2005), Gyeongju, Korea, 30 May - 4 June 2005 (published in AIP Conf.Proc., **805**, 48-54 (2006)(hep-ph/0509105); H. Baer and X. Tata, *Physics at the Large Hadron Collider* (Indian National Science Academy, A Platinum Jubilee Special Issue) (Editors: A. Datta , B. Mukhopadhyaya and A. Raychaudhari, Springer,2009); G. Bertone, D. Hooper and J. Silk, Phys. Rept. **405**, 279 (2005), L. Roszkowski, Pramana **62**, 389 (2004).
- [11] M. Drees and M. Nojiri, Phys. Rev. D **47**, 376 (1993).
- [12] <http://lepsusy.web.cern.ch/lepsusy/>.
- [13] Utpal Chattapadhyay, Debottam Das, Amitava Datta and Sujoy Poddar, Phys. Rev. D **76**, 055008 (2007).
- [14] J. R. Ellis, K. A. Olive and Y. Santoso, New J. Phys. **4**, 32 (2002); J. Ellis, K. Olive, Y. Santoso and V. Spanos, Phys. Lett. B **565**, 176 (2003); H. Baer and C. Balazs, JCAP **0305**, 006 (2003); A. Djouadi, M. Drees and J. L. Kneur, J. High Energy Phys. **0603**, 033 (2006).

- [15] J. M. Frere, D. R. T. Jones and S. Raby Nucl. Phys. B **222**, 11 (1983); J.A. Casas, A. Lleyda and C. Munoz Nucl. Phys. B **471**, 3 (1996).
- [16] J. R. Ellis, T. Falk and K. A. Olive, Phys. Lett. B **444**, 367 (1998), J. R. Ellis, T. Falk, K. A. Olive and M. Srednicki, Astropart. Phys. **13**, 181 (2000) [Erratum-ibid. **15**, 413 (2001)]; A. Lahanas, D. V. Nanopoulos and V. Spanos, Phys. Rev. D **62**, 023515 (2000); R. Arnowitt, B. Dutta and Y. Santoso, Nucl. Phys. B **606**, 59 (2001); T. Nihei, L. Roszkowski and R. Ruiz de Austri, J. High Energy Phys. **0207**, 024 (2002).
- [17] Nabanita Bhattacharyya, Amitava Datta and Sujoy Poddar, Phys. Rev. D **78**, 075030 (2008).
- [18] T. Sjostrand, P. Eden, C. Friberg, L. Lonnblad, G. Miu, S. Mrenna and E. Norrbin, Comp. Phys. Comm. **135**, 238 (2001); For a more recent version see, J. High Energy Phys. **0605**, 026 (2006).
- [19] D. Acosta, CMS Physics Technical Design Report, Vol-I, 2006.
- [20] D. Feldman, Z. Liu and P. Nath, Phys. Rev. D **78**, 083523 (2008); K. Kadota and J. Shao, Phys. Rev. D **80**, 115004 (2009); S. Bhattacharya, U. Chattopadhyay, D. Choudhury, D. Das and B. Mukhopadhyaya, Phys. Rev. D **81**, 075009 (2010).
- [21] See, *e.g.*, A.Pukhov, CalcHEP—a package for evaluation of Feynman diagrams and integration over multi-particle phase space (hep-ph/9908288). For the more recent versions see: <http://www.ifh.de/pukhov/calchep.html>.
- [22] CMS Technical Design Report, Volume II: Physics performance, A. B. Balantekin *et al.* (The CMS Collaboration), J. High Energy Phys. **0605**, 026 (2007).
- [23] M. Mangano *et al.*, J. High Energy Phys. **0307**, 001 (003).
- [24] G. Dedgassi, S. Heinemeyer, W. Hollik, P. Slavich and G. Weiglein, Eur. Phys. J. C **28**, 133 (2003); B. Allanach, A. Djouadi, J. Kneur, W. Porod and P. Slavich, J. High Energy Phys. **0409**, 044 (2004); S. Heinemeyer, W. Hollik and G. Weiglein, Phys. Rep. **425**, 265 (2006); S. Heinemeyer, Int. J. Mod. Phys. A **21**, 2659 (2006).
- [25] W. Beenakker, R. Hopker, M. Spira and P. M. Zerwas, Nucl. Phys. B **492**, 51 (1997).

- [26] M. Drees and M. Nojiri, Phys. Rev. D **47**, 376 (1993); H. Baer and M. Brhlik, Phys. Rev. D **57**, 567 (1998); H. Baer, M. Brhlik, M. Diaz, J. Ferrandis, P. Mercadante, P. Quintana and X. Tata, Phys. Rev. D **63**, 015007 (2001); J. Ellis, T. Falk, G. Ganis, K. Olive and M. Srednicki, Phys. Lett. B **510**, 236 (2001); L. Roszkowski, R. Ruiz de Austri and T. Nihei, J. High Energy Phys. **0108**, 024 (2001); A. Djouadi, M. Drees and J. L. Kneur, J. High Energy Phys. **0108**, 055 (2001); A. Lahanas and V. Spanos, Eur. Phys. J. C **23**, 185 (2002).
- [27] P. Nath and R. Arnowitt, Phys. Rev. Lett. **70**, 3696 (1993).
- [28] A. Djouadi, M. Drees and J. Kneur, Phys. Lett. B **624**, 60 (2005).
- [29] H. Baer, A. Mustafayev, E. Park and X. Tata, J. High Energy Phys. **0805**, 058 (2008); P. Bandyopadhyay, A. Datta and B. Mukhopadhyaya, Phys. Lett. B **670**, 5 (2008); U. Chattopadhyay and D. Das Phys. Rev. D **79**, 035007 (2009); L. Roszkowski, R. Austri, R. Trotta, Y. Tsai and T. A. Varley, e-Print: arXiv:0903.1279 [hep-ph]; S. Bhattacharya, U. Chattopadhyay, D. Choudhury, D. Das and B. Mukhopadhyaya, Phys. Rev. D **81**, 075009 (2010).
- [30] A. Datta, A. Datta, M. Drees and D. P. Roy, Phys. Rev. D **61**, 055003 (2000).
- [31] A. Datta, S. Maity and A. Datta, J. Phys. G **27**, 1547 (2001).
- [32] A. Datta and A. Samanta, Phys. Lett. B **607**, 144 (2005).
- [33] M. Claudson, L. J. Hall and I. Hinchliffe, Nucl. Phys. B **228**, 501 (1983); A. Kusenko and P. Langacker, Phys. Lett. B **391**, 29 (1997).
- [34] E. Barberio *et al.* . [Heavy Flavor Averaging Group], arxiv:0808.1297 [hep-ex].
- [35] M. Misiak *et al.* , Phys. Rev. Lett. **98**, 022002 (2007).
- [36] N. Chen, D. Feldman, Z. Liu and P. Nath, Phys. Lett. B **685**, 174 (2010).
- [37] K. I. Okumura and L. Roszkowski, Phys. Rev. Lett. **92**, 161801 (2004); M. E. Gomez, T. Ibrahim, P. Nath and S. Skadhauge, Phys. Rev. D **74**, 015015 (2006).